Combined Simulation of Airflow, Radiation and Moisture Transport for Heat Release from Human Body

Shuzo Murakami[1], Shinsuke Kato[1], and Jie Zeng[2]

[1]Institute of Industrial Science, University of Tokyo, Japan
[2]Graduate school, University of Tokyo, Japan

ABSTRACT

As the thermal sensation of humans depends directly on heat transfer characteristics between the body surface and the surrounding environment, it is very important to clarify the heat transfer characteristics of a human body surface in detail. This paper describes a combined numerical (NOTE 1) simulation system of airflow, thermal radiation and moisture transport based on a human thermo-physiological model used to examine the total (sensible + latent) heat transfer characteristics of a body surface. The human body is assumed to be naked (NOTE 2). Flow, temperature and moisture fields are investigated with 3-dimensional Computational Fluid Dynamics (CFD). The CFD uses a low-Reynolds-number type k- ϵ turbulence model, with the generalized curvilinear coordinate system (Boundary Fitted Coordinates) to represent the complicated shape of a human body. Thermal radiation is calculated by means of Gebhart's absorption factor method, and the view factors are obtained by the Monte Carlo method. Gagge's two-node model is included to simulate the metabolic heat production and the thermoregulatory control processes of a human body. However, heat loss due to respiration is specified in advance and is not included in the simulation directly. The prediction results agree well with those of an actual human body in a similar situation.

KEY WORDS

CFD, Convective heat transfer, Radiative heat transfer, Moisture transport, Thermal comfort

INTRODUCTION

CFD technique has been greatly developed in recent years. It is now possible for HVAC researchers to numerically investigate complicated indoor climates with sufficient accuracy and acceptable CPU time (Murakami 1992; Kato et al. 1994). Moreover, coupled simulation of CFD and thermal radiation (NOTE 1) has also been developed (Murakami et al. 1992). This is of great advantage in analyzing thermal comfort of a human body since thermal radiation plays an important role in the thermal sensation of humans.

One of the most important research targets in the field of HVAC is to investigate thermal sensation. These studies used to be carried out by means of experiments. However, recently researchers have also begun to numerically analyze thermal sensation on the basis of coupled simulation of CFD and radiation (Murakami et al. 1997). Due to the complicated shape and thermo-physiological properties of a human body, it is very difficult to include these factors totally into the numerical simulation of indoor climate. Thus, in many cases the human body is considered only as a heat source. In a few studies, a simply-shaped human body is arranged. It is often assumed simply as a rectangle. And it is also simply assumed that the body surface has uniform temperature or uniform heat production without considering the thermoregulatory processes of the body in response to the environment. To the author's knowledge, there is no numerical study which takes thermoregulatory sweating into account. People need to improve the accuracy of the prediction results which are given through these simplifications. Thermal sensation is highly dependent on the local heat transfer characteristics of the body surface. The existence of the human body and the metabolic heat production of the body have great influence on the microclimate around the body. On the other hand,

the local heat transfer characteristics of a body greatly depends on the local properties of the microclimate. Thus it is highly important to correctly analyze the interaction between a human body and the microclimate around it.

This study develops a combined numerical simulation system of airflow, moisture transport (CFD), and thermal radiation based on a human thermo-physiological model reproducing the complicated shape of the body. This system is applied successfully to examine the total (sensible + latent) heat transfer characteristics of a human body. Therefore this system will become a key technique for precisely predicting the thermal sensation of humans.

FLOWFIELD ANALYZED

The flowfield analyzed is shown in Figure 1. As stated above, the aim of this paper is to develop a combined numerical simulation system to investigate the total (sensible + latent) heat transfer characteristics of a human body. A naked human body (manikin) (NOTE 2) standing in a stagnant environment is the target of the simulation in this paper. The metabolic heat production M is set as 1.7Met (100.4W/m^2). The room is air-conditioned with a displacement ventilation system in order to remove the heat production from the manikin (supply temperature: 22℃, supply velocity: 0.12m/s, air flow rate: 57m^3/h, air change rate: 3.7ACH). The wall around the room is adiabatic for heat and the same for moisture. The shape of the manikin is slightly simplified from that of a real human body (Figure 1), with feet and arms put together close to the body.

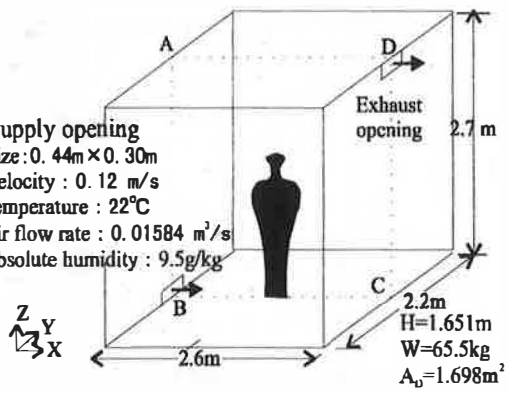

Figure 1 Flowfield analyzed

The manikin has the standard height and weight of Japanese male adult.

COMBINED NUMERICAL SIMULATION SYSTEM

As shown in Figure 2, the combined numerical simulation system consists of two parts. The first one is to simulate the internal heat transfer inside the human body surface based on a human thermo-physiological model. Here, the heat loss through respiration is assumed to be released directly into the environment with no influence on the atmosphere around the human body. Heat loss rate through respiration Q_{res} is specified as 8.7W/m^2 in advance from Equation A1 (Table A1), by assuming the body is in a uniform environment (T_a=26 ℃, P_a=1500kPa). Thus the total (sensible + latent) heat loss rate from skin Q_{sk} can be obtained as 91.7W/m^2 (=100.4—8.7), by excluding Q_{res} from the metabolic heat production M. The second part of the simulation is to calculate the heat transfer between the body surface and the surrounding environment by means of a coupled simulation of airflow, radiation and moisture transport. The two parts are combined at body surface through surface temperature and heat balance equation.

Human Thermo-physiological Model

Many human thermo-physiological models, including some elaborate multi-node models, were developed during the 1970s and 1980s (Fanger 1970; Stolwijk 1971; Gagge et al. 1972; Gordon et al. 1976; Gagge et al 1986). Among others Fanger's model and Gagge's two-node model are widely applied for evaluating thermal sensation, taking advantage of their well-balanced performance and simplicity (ASHRAE handbook 1993; Yokoyama et al. 1994). We also adopt these two models and examine their adaptability in our numerical simulation system. By comparing the results obtained from these two models, it becomes clear that Gagge's two-node model has wider adaptability, particularly in simulating sweating (Zeng et al. 1998). Therefore this paper shows the results given from the two-node model. Both Fanger's model and the two-node model, which deal with whole-body heat balance rather than local balance,

should be applied to the analysis of the whole body; however this study applied them locally, i.e. to each part of the body. The issues concerning the local application of these models will be discussed later.

Boundary Conditions of Body Surface

The Appendix describes the derivation of the boundary conditions for human body surface based on the two-node model. Sweat rate generated from the skin m_{sk} is calculated by using the two-node model. This becomes the boundary condition of the body surface for solving the moisture transport equation. Sensible heat loss from skin Q_t becomes the boundary condition of the human body surface for coupled simulation of heat convection and radiation.

Combined Simulation Method

Absolute humidity X is used to represent the moisture transport. The transport equation is shown in Equation 1.

Table 1 Numerical methods

Turbulence model	Low-Reynolds-number type k - ε model (Launder-Sharma Type)
Numerical schemes	Space difference: hybrid
Grid system	Computational domain is discretized into 163,008 cells for CFD and 2232 cells for radiation with BFC. The y^+ of the first cell near body and wall surface is less than 5. Considering the symmetrical property of the flowfield, half of the space is calculated.

Table 2 Boundary conditions

Supply opening	$U_{in}=0.12$ m/s, $T_{in}=22$ ℃, $X_{in}=9.5$g/kg, $k_{in}=0.002U_{in}^2$, $\varepsilon_{in}=k_{in}^{3/2}/(0.3D)$, $D=0.2m$
Exhaust opening	U, k, ε, T, X: free slip
Wall boundary	U, k, ε : $U_w=0$, $k_w=(\partial k/\partial x)_w=0$, $\tilde{\varepsilon}_w=0$
	Moisture: $(\partial X/\partial y)_w=0$ (adiabatic wall) $m_{sk}=-\lambda_x(\partial X/\partial y)_w$ (body surface)
	Temperature: based on heat balance equation $Q_g=Q_{cd}+Q_r+Q_{cv}$ ① adiabatic wall: $Q_{cd}=0$, $Q_g=0$ body surface: $Q_{cd}=0$, $Q_g=Q_t$ ② $Q_{cv}=-\lambda(\partial T/\partial y)_w=\lambda(T_w-T_l)/y_l$ ③ $Q_r=\sigma\varepsilon_i T_i^4-\sum_{j=1}^{N}B_{ij}\sigma\varepsilon_i T_j^4$ $\varepsilon=0.98$ (body), 0.95 (wall), 0.0 (opening and symmetry surface)

$$\frac{\partial \rho X}{\partial t}+\nabla(\rho U X)=\nabla\left[\left(\lambda_x+\frac{\mu_t}{\sigma_x}\right)\nabla X\right] \qquad (1)$$

Here, moisture conductive coefficient λ_x is 3.082×10^{-5}kg/(m · s) (Nakayama 1987). Turbulent Schmidt number σ_x is assumed to be 1.0.

Numerical methods and boundary conditions for CFD are shown in Tables 1 and 2. Flow, temperature and moisture fields are calculated with 3-D CFD. The CFD uses the Launder-Sharma type low-Reynolds-number k- ε turbulence model (Launder and Sharma 1974). The thermal radiation is calculated by means of Gebhart's absorption factor method (Gebhart 1954), and the view factors are obtained by the Monte Carlo method (Omori et al. 1990).

Figure 2 illustrates the flow chart of

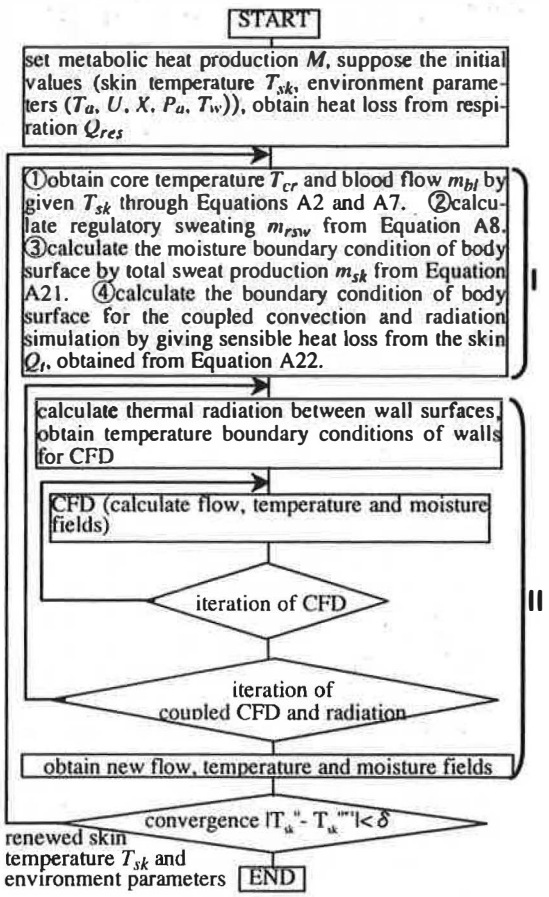

I : internal heat transfer inside body surface.
II : interactive heat transfer between body surface and environment

Figure 2 Flow chart of combined simulation of airflow, radiation, and moisture transport

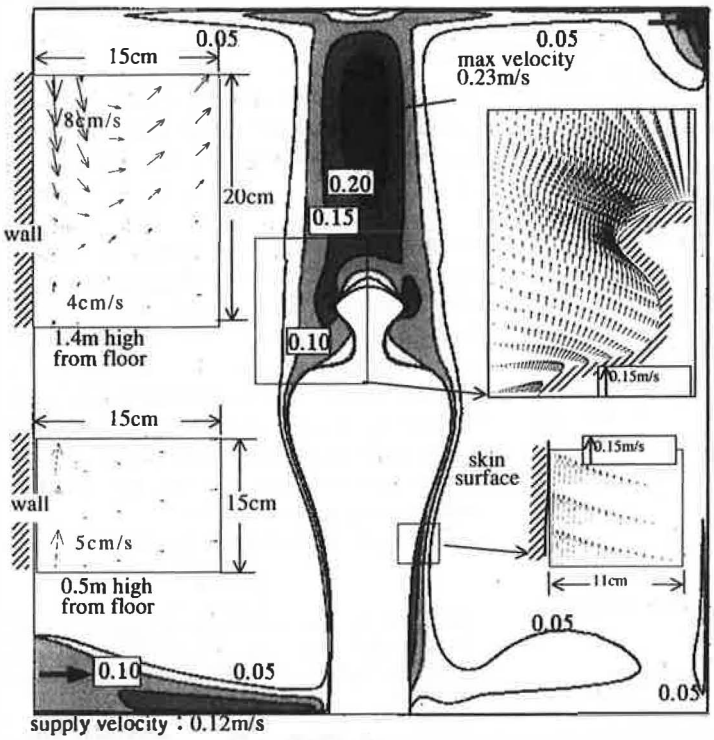

Figure 3 Predicted velocity field (scalar and vector) (Section ABCD, m/s)

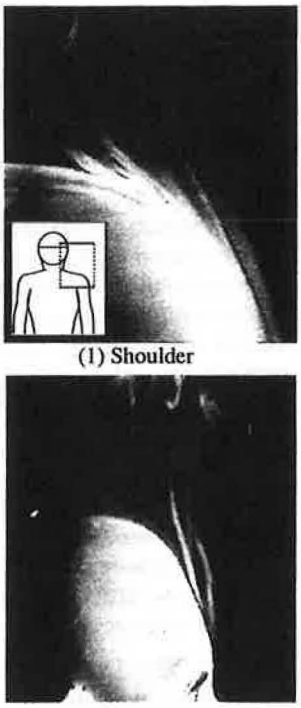

Figure 4 Flow visualization by experiment

the combined simulation of airflow, moisture transport, and radiation based on the two-node model. For the internal heat transfer inside the body surface, sweat rate m_{sk}, and sensible heat loss from skin Q_t can be calculated by given skin temperature T_{sk} and the environment parameters (T_a, U, X, P_a, T_w). The obtained values are used as boundary conditions for the combined simulation of airflow, radiation and moisture transport, i.e. interactive heat transfer between the human body and its surrounding environment. Through this process, skin temperature T_{sk} and the environment parameters are renewed. The renewed values are fed back to the internal heat transfer part as calculation conditions. The iteration will be continued until each variation becomes convergent.

RESULTS AND DISCUSSION

Velocity Distribution

The velocity distribution of Section ABCD (cf. Figure 1) is shown in Figure 3. It is clear that a blanket of warm rising air is generated around the human body, whilst the flowfield apart from the manikin is almost stagnant. When the rising air passes from the neck to the head region, it is accelerated due to the contraction following the change of the body shape. In the upper region over the manikin, a rising thermal plume is observed. The authors also carried out experiments of flow visualization using both an experimental thermal manikin and a real human body. Figure 4 shows flow patterns near the shoulder and above the head in the experiment. The simulated flow pattern agrees very well with the experimental results. The rising stream over the head reaches a maximum velocity of 0.23m/s in the numerical simulation. The predicted value agrees well with the measurements carried out by the authors, using a real human body (0.20m/s) and a thermal manikin (0.21m/s). The results are also consistent with a previous experiment (Homma et al. 1988). The thickness of the velocity boundary layer around the manikin surface increases with respect to height, similar to the flow pattern along a vertical heated flat plate (Kato et al. 1993).

Air Temperature Distribution

Figure 5 shows the air temperature

distribution around the manikin. A vertical temperature gradient is formed in the room due to the displacement ventilation system. There is clearly a temperature difference between the feet and head levels (3-4℃). The vertical temperature gradient, however, is not so steep compared with the previous result which was given from the analysis where convection and radiation were not coupled and only the convection was dealt with (Murakami et al. 1997). This result is caused by thermal radiation, which decreases surface temperature difference between the surrounding walls. The ceiling, floor and other walls are assumed to be adiabatic here. As a result, air temperature has a tendency to become uniform. In the upper region of the room above the manikin, air temperature is higher and almost uniform at 27℃.

Distribution of Absolute Humidity and Relative Humidity

Figures 6 and 7 show distribution of absolute humidity and relative humidity respectively. Moisture generated from manikin goes up with the rising stream around body surface. Consequently, absolute humidity in the upper part of the space is higher than that in the lower part. As relative humidity depends on temperature, it has higher values near the supply opening, where the temperature is low. Relative humidity is also distributed pretty uniformly from 45% to 50%, through the entire room space.

Wall Surface Temperature

Figure 8 shows surface temperature distribution of the surrounding walls. The surrounding adiabatic walls gain heat from the manikin by radiation, and then lose it to the air by convection. Thus wall surface temperatures are generally about 0.3 ℃ higher than the air temperature. Radiative heat transfer also occurs between the walls, due to temperature difference between the wall surfaces. This causes uniform wall surface temperature distribution.

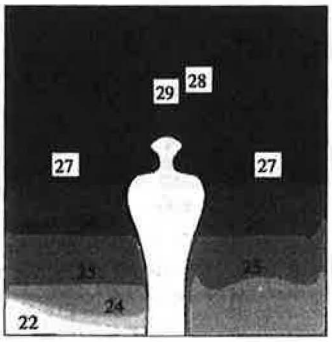

Figure 5 Air temperature (Section ABCD, ℃)

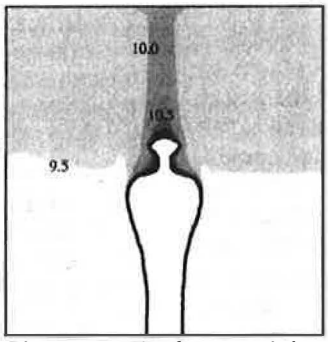

Figure 6 Absolute humidity (g/kg)

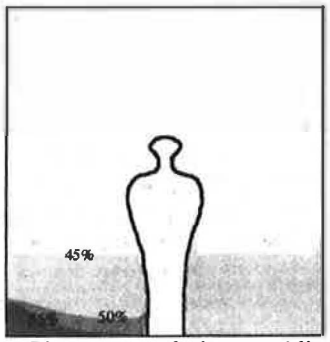

Figure 7 Relative humidity

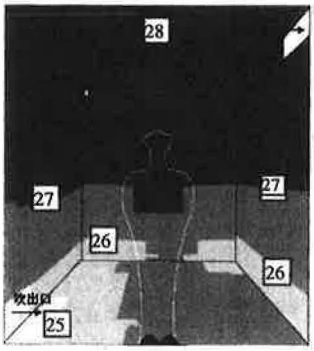

Figure 8 Wall surface temperature (℃)

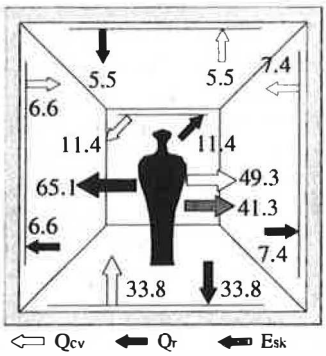

Figure 9 Heat balance between human body and surrounding walls (W)

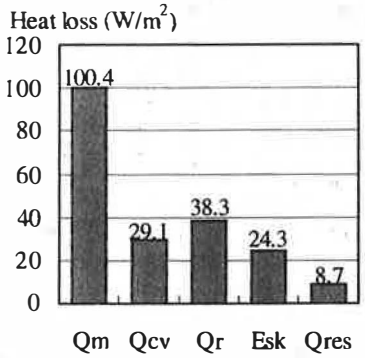

Figure 10 Heat loss from human body (W/m²)

Heat Balance between Manikin and Surrounding Walls

Figure 9 shows the heat balance of the manikin and the surrounding walls. The average heat loss characteristics of the human body are shown in Figure 10. One of the main purpose of this paper is to clarify the characteristics of the heat loss from a standing human body with activity level of 1.7Met (100.4W/m^2) in a stagnant environment. Heat loss by radiation, convection, evaporation and respiration are calculated as 65.1W (38.3W/m^2), 49.3W (29.1W/m^2), 41.3W (24.3W/m^2) and 14.8W (8.7W/m^2) respectively. Floor temperature is the lowest, about 1.0℃ lower than that of the other walls (cf. Figure 8). Thus, the floor gains the largest radiative heat at about 33.8W from the manikin and walls as is shown in Figure 9. On the contrary, the ceiling has the highest temperature; it releases heat by radiation to the walls and gains heat from the air by convection.

Temperature of Manikin Skin Surface

The temperature of the manikin skin surface is shown in Figure 11(1). It generally ranges from 33.0 to 34.0℃. It decreases below 29.0℃ at the feet, and increases above 34 ℃ at the neck. Experimental results (Torikai et al. 1992) show a similar tendency of temperature distribution at the skin surface of a real human body. The mean skin surface temperature is calculated at 33.3℃. This value is slightly lower than that of a human body in the state of physiological thermal neutrality (33.7℃).

Convective Heat Transfer Characteristics of Manikin Surface

Figure 11(2) and (3) illustrate the convective heat transfer rate and heat transfer coefficient of the manikin skin surface. Both distribution patterns are almost similar to each other. The values are larger at the feet because of the thin boundary layer there. They become low with respect to the height of manikin. The convective heat transfer rate ranges from 20.0 to 40.0W/m^2. The convective heat transfer coefficient ranges from 3.0 to 4.0W/(m^2·K). It increases to 7.0W/(m^2·K) at the feet. The mean convective heat transfer coefficient is obtained as 4.3W/(m^2·K). The results of mean value and distribution characteristics of convective heat transfer coefficient agree well with previous experiments (Nielsen and Pedersen 1952; Rapp 1973; ASHRAE handbook 1993).

Radiative Heat Transfer Characteristics of Manikin Surface

Figure 11(4) shows radiative heat transfer rate of manikin surface. As there is no large temperature difference between the surrounding walls, it ranges pretty uniformly from 30.0 to 40.0W/m^2. The feet, however, have slightly lower values due to the low manikin surface temperature. The heat transfer by radiation is larger than that by convection on average (cf. Figures 11(2) and (4)).

Figure 11(5) shows the distribution of mean radiative temperature (NOTE 3) of manikin surface. It distributes almost uniformly from 27.0 to 28.0℃. At the left and right sides of the manikin, mean radiative temperature is low, due to the large view factors of this position towards the floor, where temperature is low.

Evaporative Heat Transfer Characteristics of Manikin Surface

Figure 11(6) shows the evaporative heat transfer rate of a body surface. It ranges from 20.0 to 30.0W/m^2. It is assumed that the total (sensible + latent) heat loss rate is the same all over the manikin surface. Consequently, the evaporative heat transfer rate decreases below 20.0W/m^2 at the feet, due to the large sensible heat transfer rate there. The value increases over 30.0W/m^2 at the shoulder. The results correspond well to experiments (Nakayama 1987).

Figure 11(7) shows the evaporative heat transfer coefficient of manikin surface. The distribution property is similar to that of the convective heat transfer coefficient. A large value appears at the feet due to the thin boundary layer there. It decreases with the height of the body. The evaporative heat transfer coefficient generally ranges from 60.0 to 80.0W/(m^2·kPa) over the manikin surface. The mean value is calculated as 70.2W/(m^2·kPa). Compared to the mean convective heat transfer coefficient, the Lewis ratio is obtained as 16.5℃/kPa, the same as the value recommended by ASHRAE (ASHRAE handbook 1993).

Skin Wettedness

Figure 11(8) shows skin wettedness of the manikin surface. As the evaporative heat transfer rate at the feet is low, skin wettedness is also low there at 0.06. This means that only diffusive evaporation occurs and regulatory sweating is not generated at the feet in this calculation condition. Skin wettedness becomes larger as the height of the body increases. It becomes the largest, over 0.18, at the shoulder. This distribution property agrees well with the actual situation of a real human body (Nakayama 1987). The mean value is 0.11. This corresponds to that of a human body in thermal neutrality with the activity level of 1.7Met.

Other Physiological Parameters of Manikin

The core temperature of the manikin is almost 36.9℃ everywhere (Figure is omitted). It is almost the same as the neutral core temperature (36.8℃). Figure 11(9) shows the skin blood flow rate of the manikin. It generally ranges from 4.0 to 6.0g/(s·m^2) over the manikin surface. The blood flow rate is below 2.0 g/(s·m^2) at the feet. It increases above 7.0g/(s·m^2) at the shoulder and the neck. This distribution property corresponds to the manikin surface temperature (cf. Figure 11(3)).

CONCLUDING REMARKS

(a) A combined numerical simulation system is developed for predicting airflow, moisture transport, and thermal radiation based on a human thermo-physiological model. This system makes it possible to investigate precisely the total (sensible + latent) heat transfer charac-

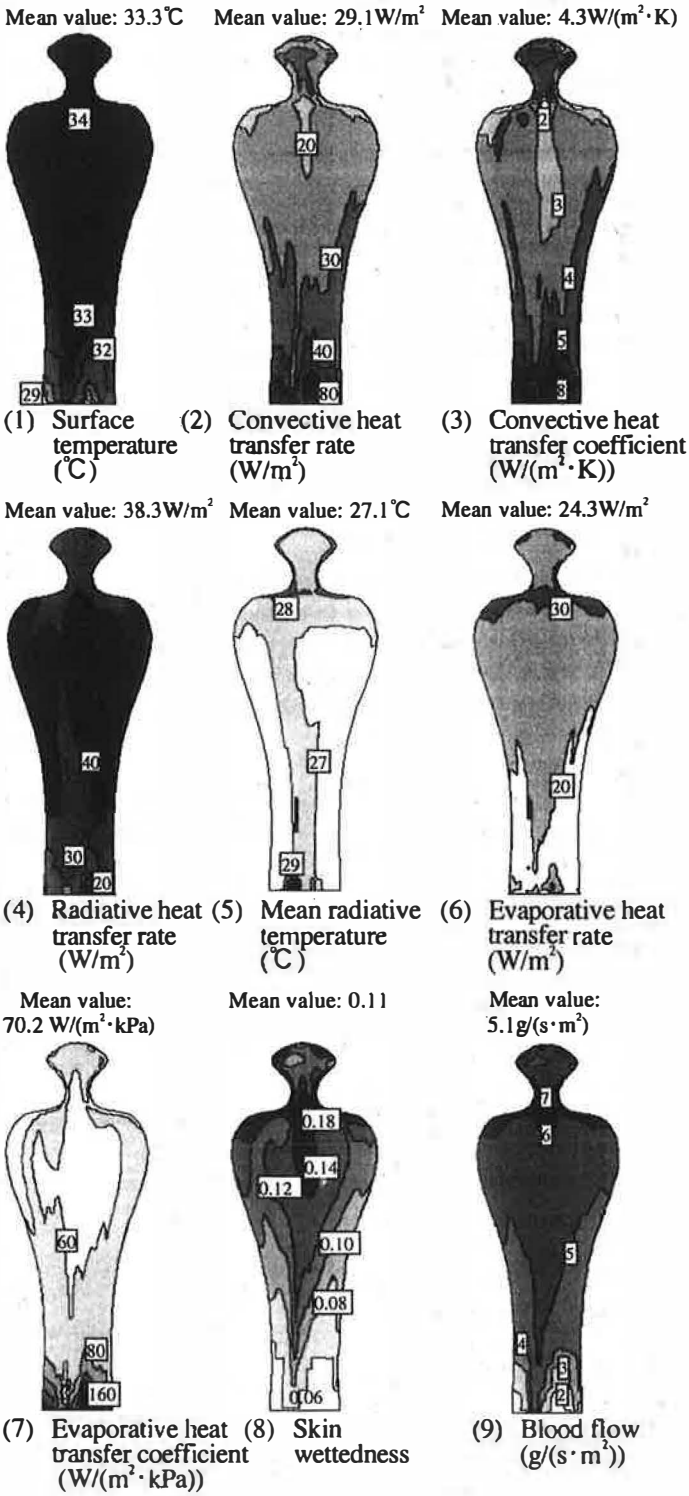

Figure 11 Thermal characteristics of body surface

teristics of the human body skin surface. The human body is naked in this study. The case with clothing will be reported in the next paper.

(b) The two-node model is used here. It was originally developed for applying to the whole body heat budget. In its original concept it was not enough possible to apply this model to analyze local heat transfer as carried out in this study. However, when adapting it locally to body surface, the obtained heat transfer characteristics of the body agree well with the actual phenomena of the real human body. The use of the two-node model locally at a body surface seems tolerable in such analyses. The multi-node model will be examined at the next stage.

(c) Thermal sensation indices, such as SET*, PMV, are to be reported in the next paper based on the results of this study. Human's thermal sensation thus can be predicted precisely by this combined numerical prediction system.

APPENDIX

Boundary conditions of body surface are derived based on the two-node model. Table A1 shows the set of equations. The two-node model (Gagge et al. 1972; Gagge et al. 1986; ASHRAE handbook 1993) represents the body as two concentric cylinders —the inner cylinder represents the body core and the outer cylinder represents the skin layer. The metabolic heat production at the core is released to the environment by two routes. The major one is to transfer heat to the skin by blood flow and heat conduction, and to be released from the skin to the environment by convection, radiation and evaporation. The minor one is a direct release to the environment through respiration (Equation A1). As shown in Equations A2 and A3, two heat balance equations for the body core and the skin layer are dealt with. Here, steady condition is assumed; thus the rates of heat storage, S_{cr}, S_{sk}, are assumed to be zero.

When the body is physiologically in the state of thermal neutrality, the mean temperatures of core $T_{cr,n}$, skin $T_{sk,n}$, and

Table A1 Derivation of boundary conditions of human body surface (following Gagge et al. 1986)

1) Heat loss from respiration Q_{res}

$$Q_{res} = 0.0014M(34.0 - T_a) + 1.73\times10^{-5}M(5.87\times10^{3} - P_a) \quad \text{A1}$$

2) Heat balance equations for body core and skin layer

$$S_{cr} = (Q_m - Q_{res}) - K(T_{cr} - T_{sk}) - c_{p,bl}m_{bl}(T_{cr} - T_{sk}) \quad \text{A2}$$

$$S_{sk} = K(T_{cr} - T_{sk}) + c_{p,bl}m_{bl}(T_{cr} - T_{sk}) - E_{sk} - (Q_{cv} + Q_r) \quad \text{A3}$$

3) Thermal neutrality for body core, skin layer, and whole body

$$T_{cr,n} = 36.8℃ \quad \text{A4} \qquad T_{sk,n} = 33.7℃ \quad \text{A5}$$

$$T_{b,n} = \beta_n T_{sk,n} + (1 - \beta_n)T_{cr,n} \quad \text{A6}$$

4) Thermo-regulatory control processes (vasomotor regulation and sweating)

$$m_{bl} = [(6.3 + 200WSIG_{cr})/(1 + 0.1CSIG_{sk})]/3600 \quad \text{A7}$$

$$m_{rsw} = 4.72\times10^{-5}WSIG_b \exp(WSIG_{sk}/10.7) \quad \text{A8}$$

$$\beta = 0.042 + 0.745/(3600m_{bl} + 0.585) \quad \text{A9}$$

5) Temperature signals

$$WSIG_{cr} = \max((T_{cr} - T_{cr,n}),0) \quad \text{A10} \qquad CSIG_{sk} = \max((T_{sk,n} - T_{sk}),0) \quad \text{A11}$$

$$WSIG_b = \max((T_b - T_{b,n}),0) \quad \text{A12} \qquad WSIG_{sk} = \max((T_{sk} - T_{sk,n}),0) \quad \text{A13}$$

$$T_b = \beta T_{sk} + (1 - \beta)T_{cr} \quad \text{A14}$$

6) Boundary conditions for solving moisture transport equation

$$E_{rsw} = m_{rsw}h_{fg} \quad \text{A15} \qquad w_{rsw} = E_{rsw}/E_{max} \quad \text{A16} \qquad E_{dif} = (1 - w_{rsw})0.06E_{max} \quad \text{A17}$$

$$w = w_{rsw} + 0.06(1 - w_{rsw}) = 0.06 + 0.94E_{rsw}/E_{max} \quad \text{A18} \qquad E_{sk} = wE_{max} \quad \text{A19}$$

$$E_{max} = \alpha_e(P_{sk,s} - P_{a,ref}) \quad \text{A20} \qquad m_{sk} = E_{sk}/h_{fg} \quad \text{A21}$$

7) Boundary conditions for coupled simulation of heat convection and radiation

$$Q_t = Q_m - Q_{res} - E_{sk} \quad \text{A22}$$

whole body $T_{b,n}$ are at their neutral values (Equations A4-A6). When the temperature deviates from neutrality, the thermoregulatory control processes (vasomotor regulation, sweating, and shivering) occur. These processes are simulated by temperature signals as shown in Equations A7 and A8. Here, temperature signals are defined in Equations A10-A13. The mean body temperature T_b is calculated from Equation A14. The ratio of skin mass to whole body mass β is calculated from Equation A9.

Evaporative heat loss by regulatory sweating E_{rsw} and skin wettedness due to regulatory sweat w_{rsw} are calculated from Equations A15 and A16 respectively by the specified regulatory sweat rate m_{rsw}. With no regulatory sweating, skin wettedness due to diffusion is approximately 0.06 for normal conditions. Then the diffusion evaporative heat loss E_{dif} is calculated from Equation A17. Total evaporative heat loss from skin E_{sk} is shown in Equation A19. Total sweat rate generated from skin m_{sk} is calculated from Equation A21. This becomes the boundary condition of the body surface for solving the moisture transport equation.

Sensible heat loss from skin Q_t is derived as Equation A22. This becomes the boundary condition of a human body surface for coupled simulation of heat convection and radiation.

NOTE 1

Here, "combined simulation" means the interactive analysis of the relationship between the indoor climate and a human body which includes the thermo-physiological model, as shown by Part I + II in Figure 2. "Coupled simulation" means the mathematical procedure for connecting CFD and radiative heat transfer, as shown by Part II in Figure 2.

NOTE 2

In a previous paper (Murakami et al. 1997) analyzing the heat transfer from a human body, the internal heat transfer inside the skin surface was not dealt with. In this case, it was not necessary to define whether the human body was naked or clothed. The boundary condition for that analysis was only the metabolic heat production. In this paper, it is necessary to define the human body as being naked because the internal heat transfer is dealt with here. The skin surface temperature T_{sk} is calculated by the interactive analysis between the skin surface and the surrounding environment. However, the effect of clothing can be modeled without difficulty by introducing the thermal and vapor resistance corresponding to the clothing following Gagge's model into the currently developed simulation system. This will be done in the next stage of this simulation.

NOTE 3

More accurately, this is specified as the plane radiative temperature, which is the average at each small plane on the body surface.

NOMENCLATURE

A_D = skin surface area, m^2
B_{ij} = Gebhart's absorption factor
$c_{p,bl}$ = specific heat of blood, 4.187kJ/(kg·K)
D = hydraulic diameter, m
E_{dif} = diffusion evaporative heat transfer rate from skin, W/m^2
E_{max} = maximum evaporative potential from skin, W/m^2
E_{rsw} = evaporative heat transfer by regulatory sweating from skin, W/m^2
E_{sk} = total evaporative heat transfer from skin, W/m^2
H = human body height, m
h_{fg} = heat of vaporization of water, 2430kJ/kg
k = turbulent energy, m^2/s^2
K = effective conductance between the core and skin, $5.28W/(m^2 \cdot K)$
M = metabolic heat production, W/m^2
m_{bl} = blood flow rate, $kg/(m^2 \cdot s)$
m_{rsw} = regulatory sweat rate from skin, $kg/(m^2 \cdot s)$
m_{sk} = sweat rate generated from skin, $kg/(m^2 \cdot s)$
P_a = water vapor pressure in ambient air, Pa (here 1500kPa)
$P_{a,ref}$ = water vapor pressure in ambient air outside the boundary layer of human body, Pa
$P_{sk,s}$ = saturated water vapor pressure at T_{sk} at skin, Pa
Q_{cd} = conductive heat transfer rate, W/m^2
Q_{cv} = convective heat transfer rate, W/m^2
Q_g = heat generation rate, W/m^2
Q_m = total heat transfer rate of human body, W/m^2
Q_r = radiative heat transfer rate, W/m^2
Q_{res} = total heat transfer rate through respiration, W/m^2
Q_{sk} = total (sensible + latent) heat transfer

rate from skin, W/m^2

Q_l = sensible heat transfer rate, W/m^2

S_{cr} = rate of heat storage in core node, W/m^2

S_{sk} = rate of heat storage in skin layer, W/m^2

T = mean temperature, K (radiation), ℃ (the other)

T_a = ambient air temperature, ℃ (here, 26℃)

T_b = mean body temperature, ℃

$T_{b,n}$ = mean body temperature at neutrality, ℃

T_{cr} = temperature of core node, ℃

$T_{cr,n}$ = neutral temperature of core node, 36.8℃

T_{sk} = temperature of skin layer, ℃

$T_{sk,n}$ = neutral temperature of skin layer, 33.7℃

T_w = wall surface temperature, ℃

U = mean velocity, m/s

W = human body weight, kg

w = skin wettedness (including diffusion and regulatory sweat)

w_{rsw} = skin wettedness due to regulatory sweat

X = absolute humidity, kg/kg

y = normal direction of wall

α_e = evaporative heat transfer coefficient, W/(m^2·kPa)

β = actual ratio of skin mass to whole body mass

β_n = ratio of skin mass to whole body mass at neutrality, 0.1 (Gagge et al (1986))

ε = dissipation rate of turbulent energy, m^2/s^3, $\tilde{\varepsilon} = \varepsilon - \nu(\partial k^{1/2}/\partial x)^2$, or surface emissivity

λ = thermal conductivity, W/(m·K)

λ_x = moisture conductive coefficient, 3.082×10^{-5}kg/(m·s)

Subscript

a: air *cr*: core node *i, j*: cell number *in*: supply opening *ref*: reference point outside boundary layer of body *sk*: skin layer *s*: saturated state *n*: thermal neutrality *w*: wall surface 1: the first cell near wall

REFERENCES

ASHRAE Fundamentals Handbook, Chapter 8, 1993

Fanger, P.O. (1970) *Thermal comfort*, Danish Technical Press.

Gagge, A.P., Stolwijk, J.A.J., and Nishi, Y. (1970) An effective temperature scale based on a simple model of human physiological regulatory response. *ASHARE Trans.*, 77(1), 247-262.

Gagge, A.P., Fobelets, A.P., and Berglund, L.G. (1986) A standard predictive index of human response to the thermal environment. *ASHARE Trans.*, 92(1), 709-731.

Gebhart, B. (1959) A new method for calculating radiant exchanges, *ASHRAE Trans.*, 65, 321-323.

Gordon, R. G., Rober, R. B. and Horvath, S. M. (1976) *IEEE Trans.*, BME-23, 434-444.

Homma, H. and Yakiyama, M. (1988) Examination of free convection around occupant's body caused by it's metabolic heat. *ASHRAE Trans.*, 94(1), 104-124.

Kato, S., Murakami, S., and Yoshie, R. (1993) Experimental and numerical study on natural convection with strong density variation along a heated vertical plate. *Proceedings of the 9th Symposium on "Turbulent Shear Flows"*, 12-5. Kyoto, Japan.

Kato, S., Murakami, S., Shoya, S., Hanyu, F., and Zeng, J. (1994) CFD analysis of flow and temperature fields in atrium with ceiling height of 130m. *ASHRAE Trans.*, 95(2).

Launder, B. E. and Sharma, B. I. (1974) Application of the energy-dissipation model of turbulence to the calculation of flow near a spinning disc. *Letters in Heat and Mass Transfer*, 1, 131-138.

Murakami, S. (1992) Prediction, analysis and design for indoor climate in large enclosures. *Proceedings of Roomvent'92*, 1-30. Denmark.

Murakami, S., Kato, S., Omori, T., Choi, D., and Kobayashi, H. (1992) *"SEISAN-KENKYU"*, 44(2), 56-63 (in Japanese).

Murakami, S., Kato, S., and Zeng J. (1997). Flow and temperature fields around human body with various room air distribution, CFD study on computational thermal manikin (Part 1). *ASHRAE Trans.*, 103(1).

Nakayama S. (1987) *Thermophysiology*. Rikougakusya (in Japanese).

Nielsen, M. and Pedersen, L. (1952) Studies on the Heat Loss by Radiation and Convection from the Clothed Human Body. *Acta, Phys. Scandinav.*, 27, 272-294.

Omori, T., Taniguchi, H., and Kudo, K. (1990) Prediction method of radiant environment in a room and its application to floor heating. *SHASE Trans.*, 42, 9-18 (in Japanese).

Rapp, G. M. (1973) Convective heat transfer and convective coefficients of nude man, cylinders and spheres at low velocities. *ASHRAE Trans.*, 2264, 75-87.

Stolwijk, J.A.J. (1971) A mathematical model of physiological temperature regulation in man. *NASA contractor report*, NASA CR-1855.

Torikai, K., Suzuki, K., and Tsutaki, S. (1992) Thermal emission from human body. *Proceedings of the 2nd JSME-KSME thermal engineering conference.*

Yokoyama, S., Ochihuji, S., and Nagano K. (1994) *Journal of the Heat Transfer Society of Japan*, 33(131), 41-50 (in Japanese).

Zeng, J., Kato, S., and Murakami, S. (1998) Coupled simulation of CFD, radiation and moisture transport for sensible and latent heat loss from human body, study of computational thermal manikin. *"SEISAN-KENKYU"*, 50(1), 78-85. (in Japanese).